Research Article

Cyclooxygenase-2–Dependent Regulation of E-Cadherin: Prostaglandin E_2 Induces Transcriptional Repressors ZEB1 and Snail in Non–Small Cell Lung Cancer

Mariam Dohadwala,[1,2,5] Seok-Chul Yang,[1,2,5] Jie Luo,[2] Sherven Sharma,[1,2,5] Raj K. Batra,[1,2,5] Min Huang,[1,5] Ying Lin,[2] Lee Goodglick,[1,4] Kostyantyn Krysan,[1,2] Michael C. Fishbein,[4] Longsheng Hong,[1,4] Chi Lai,[4] Robert B. Cameron,[1,3] Robert M. Gemmill,[6] Harry A. Drabkin,[6] and Steven M. Dubinett[1,2,4,5]

[1]Lung Cancer Research Program of the University of California at Los Angeles Jonsson Comprehensive Cancer Center and Departments of [2]Medicine, [3]Surgery, and [4]Pathology and Laboratory Medicine, David Geffen School of Medicine at University of California; [5]VA Greater Los Angeles Health Care Center, Los Angeles, California and [6]Division of Medical Oncology, University of Colorado Health Science and Cancer Centers, Denver, Colorado

Abstract

Elevated tumor cyclooxygenase-2 (COX-2) expression is associated with tumor invasion, metastasis, and poor prognosis in non–small cell lung cancer (NSCLC). Here, we report that COX-2-dependent pathways contribute to the modulation of E-cadherin expression in NSCLC. First, whereas genetically modified COX-2-sense (COX-2-S) NSCLC cells expressed low E-cadherin and showed diminished capacity for cellular aggregation, genetic or pharmacologic inhibition of tumor COX-2 led to increased E-cadherin expression and resulted in augmented homotypic cellular aggregation among NSCLC cells *in vitro*. An inverse relationship between COX-2 and E-cadherin was shown *in situ* by double immunohistochemical staining of human lung adenocarcinoma tissue sections. Second, treatment of NSCLC cells with exogenous prostaglandin E_2 (PGE_2) significantly decreased the expression of E-cadherin, whereas treatment of COX-2-S cells with celecoxib (1 μmol/L) led to increased E-cadherin expression. Third, the transcriptional suppressors of E-cadherin, ZEB1 and Snail, were up-regulated in COX-2-S cells or PGE_2-treated NSCLC cells but decreased in COX-2-antisense cells. PGE_2 exposure led to enhanced ZEB1 and Snail binding at the chromatin level as determined by chromatin immunoprecipitation assays. Small interfering RNA–mediated knockdown of ZEB1 or Snail interrupted the capacity of PGE_2 to down-regulate E-cadherin. Fourth, an inverse relationship between E-cadherin and ZEB1 and a direct relationship between COX-2 and ZEB1 were shown by immunohistochemical staining of human lung adenocarcinoma tissue sections. These findings indicate that PGE_2, in autocrine or paracrine fashion, modulates transcriptional repressors of E-cadherin and thereby regulates COX-2-dependent E-cadherin expression in NSCLC. Thus, blocking PGE_2 production or activity may contribute to both prevention and treatment of NSCLC. (Cancer Res 2006; 66(10): 5338-45)

Requests for reprints: Steven M. Dubinett, David Geffen School of Medicine at University of California at Los Angeles, 37-131 CHS, 10833 Le Conte Avenue, Los Angeles, CA 90095. Phone: 310-794-6566; Fax: 310-267-2829; E-mail: sdubinett@mednet.ucla.edu.

doi:10.1158/0008-5472.CAN-05-3635

Introduction

Lung cancer is the most common cause of cancer-related mortality in men and women in the United States, accounting for ~30% of all such deaths per year (1). Despite focused research in conventional therapies and considerable advances in the understanding of the molecular carcinogenesis of lung cancer, the 5-year survival rate for all lung cancer patients remains ~15%. Because most lung cancer patients eventually succumb to widespread metastases (2), the identification of mechanisms regulating this process is of utmost importance.

Tumor cyclooxygenase-2 (COX-2) and its metabolite prostaglandin E_2 (PGE_2) play important roles in regulating diverse cellular functions under physiologic and pathologic conditions (1–3). COX-2, the inducible isoenzyme, is constitutively overexpressed in a variety of malignancies, including colon, gastric, esophageal, prostate, pancreatic, breast, and lung carcinomas (2–5). We and others have reported previously that COX-2 is overexpressed in human non–small cell lung cancer (NSCLC; refs. 5–7) and that inhibition of COX-2 leads to tumor reduction *in vivo* in murine lung cancer models (8, 9). COX-2 activity can be detected throughout the progression of a premalignant lesion to the metastatic phenotype (6). Compared with the primary tumor, higher COX-2 expression was observed in lung adenocarcinoma lymph node metastases (6). Studies indicate that overexpression of COX-2 is associated with angiogenesis (9, 10), decreased host immunity (5, 8, 11, 12), and enhanced invasion and metastasis (13–16). Thus, because COX-2 can affect multiple mechanistic pathways in lung cancer carcinogenesis, it has been suggested to play a multifaceted role in conferring the malignant and metastatic phenotypes (17, 18).

Although multiple genetic alterations are necessary for lung cancer invasion and metastasis, COX-2 may be a central element in orchestrating this process (14, 15, 17, 18). Previously, we reported that the COX-2-dependent invasive capacity in NSCLC was due to PGE_2-mediated regulation of CD44 and matrix metalloproteinase-2 (MMP-2; ref. 15). Here, we focus on an additional aspect of this important process. In the present study, we define a new pathway whereby COX-2/PGE_2 regulates E-cadherin expression in NSCLC.

The complex events associated with tumor cell invasion and metastasis include the active movement of cells across the extracellular matrix (ECM) and spread to distant organ sites (19). Disruption of normal cell-cell adhesion contributes to the enhanced migration and proliferation of tumor cells leading to invasion and metastasis (19, 20). This disruption can be achieved

by down-regulating the cadherin or catenin family members or by activation of signaling pathways that prevent the assembly of cell-cell adheren junctions (19). Thus, ECM and cell-cell adhesion represent significant barriers to tumor cell metastasis.

The E-cadherin-catenin complex is critical for intercellular adhesiveness and maintenance of normal tissue architecture (19, 21, 22). Reduction of E-cadherin has been previously linked to tumor invasion, metastasis, and unfavorable prognosis (21, 23, 24). Loss of E-cadherin together with increased COX-2 expression has been documented in familial adenomatous polyposis (16). However, the pathways whereby COX-2 regulates E-cadherin in NSCLC have not been previously defined. Here, we report that tumor COX-2 suppresses E-cadherin expression via PGE_2-mediated induction of the transcriptional repressors ZEB1 and Snail. Immunohistochemical staining of lung adenocarcinoma tissue sections confirm that these relationships exist *in situ*. This is the first report implicating COX-2/PGE_2-dependent regulation of E-cadherin transcriptional repressors in cancer.

Materials and Methods

Reagents and NSCLC cell lines. 16,16-Dimethyl-PGE_2 was purchased from Cayman Chemical (Ann Arbor, MI). Other reagents were purchased from Sigma Chemical (St. Louis, MO) unless otherwise specified. NSCLC cells, A549 (human lung adenocarcinoma) and NCI-H157 (squamous cell carcinoma), were obtained from American Type Culture Collection (Rockville, MD) and the National Cancer Institute, respectively. COX-2 sense (COX-2-S) and COX-2 antisense (COX-2-AS) oriented and pLNCX (vector alone) clones were generated for A549 and H157 cell lines using retroviral transfection as described previously (14, 15). Briefly, for each cell line, ~10-fold higher levels of COX-2 expression and PGE_2 production were noted in COX-2-S compared with parental or vector controls (14). In contrast, COX-2-AS cells produced 4-fold less COX-2 and PGE_2 (14). These cells were then expanded for further studies. The following cell line terminology is used in the text: (*a*) A549-S and H157-S are the cell lines transfected with COX-2 in the sense orientation, (*b*) A549-AS and H157-AS are the cell lines transfected with COX-2 in antisense orientation, and (*c*) A549-V and H157-V are the cells transfected with the expression vector pLNCX alone. E-cadherin-overexpressing cells were generated as follows: (*a*) wild-type E-cadherin cDNA pcDNA3.1 (a generous gift from A.S.T. Wong and B.M. Gumbiner, University of Virginia, Charlottesville, VA) was excised from the plasmid with *Hin*dIII and *Xba*I and subcloned into pCR3.1 vector (Invitrogen, Carlsbad, CA). (*b*) A 2.7-kb E-cadherin cDNA was further excised from pCR3.1 construct with *Pme*I and *Hin*dIII and subcloned into the retrovirus vector pLHCX (Clontech, Mountain View, CA), which contains the cytomegalovirus promoter for controlling transcription of the cDNA insert and hygromycin (Mediatech, Herndon, VA) resistance gene for selection. (*c*) The constructs were verified by restriction endonuclease digestion. Sense (E-cadherin-S) and antisense (E-cadherin-AS) oriented expression vectors were prepared as described previously (14). For virus production, 70% confluent 293T cells were transfected with E-cadherin-S, E-cadherin-AS, and pLHCX (vector alone). Tumor cells were then transduced with high titer producing E-cadherin-S, E-cadherin-AS, and pLHCX virus. Following transduction, the tumor cells were characterized by Western blot for E-cadherin expression.

Western blot analysis. NSCLC cells were washed with PBS and whole-cell lysate was prepared with modified radioimmunoprecipitation assay buffer at 4°C for 15 minutes. The cell lysates were centrifuged at 13,000 rpm for 10 minutes and the supernatant was collected. Protein concentration was measured with a protein assay reagent (Bio-Rad, Hercules, CA). Proteins for E-cadherin (20 μg) and ZEB1 (50 μg) were resolved by SDS-PAGE and analyzed by Western blot using polyvinylidene difluoride membranes (Millipore, Bedford, CA) according to the manufacturer's instructions. Membranes were blocked with 5% nonfat dry milk in TBS plus 0.1% Tween 20 (TBST). The membranes were probed with anti-E-cadherin antibody (BD Biosciences PharMingen/Transduction Laboratories, San Jose, CA) at 1:2,500 dilution and anti-ZEB1 antibody (Santa Cruz Biotechnology, Santa Cruz, CA) at 1:1,000 dilution in TBST containing 1.0% nonfat dry milk. The membranes were developed by the enhanced chemiluminescence system (Amersham Pharmacia Biotech, Piscataway, NJ) and exposed to X-ray film (Optimum Brand X-ray Film). Equal loading of samples was confirmed by probing the membranes with β-actin or glyceraldehyde-3-phosphate dehydrogenase (GAPDH) antibody.

Cell aggregation assay. Aggregation assays were done as described previously with minor modification (25). Briefly, cells grown to 80% confluence in RPMI/10% fetal bovine serum (FBS) were washed with HCMF (10 mmol/L HEPES-buffered Ca^{2+},Mg^{2+}-free Hanks' solution). To obtain a dispersed cell suspension with intact E-cadherin, the cells were treated with 0.01% trypsin and 5 mmol/L $CaCl_2$ in HCMF at 37°C for 15 minutes on a gyratory shaker at 75 rpm. Following FBS addition to 20% to quench trypsin, cells were pelleted at 1,000 rpm for 5 minutes and the pellet was resuspended in HCMF containing 1% BSA. Cells (5×10^4) in 0.5 mL HCMF were placed into wells of a 24-well and incubated for 1 hour at 37°C gyratory shaker at 75 rpm. The efficiency of cell aggregation was assessed using a Leica DM IRB microscope attached to Optronics Fire Magnafire Digital Camera (Leica, Wetzlar, Germany). The degree of cell aggregation was determined according to the decrease in particle number: % Aggregation = 1 − [number of particles Px (at time $t = x$) / initial particle number P0] × 100. At least three independent experiments were done for each group (COX-2-S, COX-2-AS, COX-2-S + E-cadherin-S, COX-2-AS + E-cadherin-Ab, and COX-2-AS + control-Ab). A minimum of five fields was scored per group in each experiment.

Total RNA preparation, cDNA synthesis, and real-time PCR. To analyze the COX-2/PGE_2-dependent regulation of E-cadherin, ZEB1, and Snail mRNA expression, total RNA from 1×10^6 COX-2-S, COX-2-AS, vector alone, and PGE_2 (10 μg/mL) vector-transfected cells was extracted using Trizol reagent according to the manufacturer's instructions (Invitrogen). The cDNA was prepared with a kit (Invitrogen) according to the manufacturer's instructions.

E-cadherin, ZEB1, and Snail mRNA levels were quantified by real-time reverse transcription-PCR (RT-PCR) using the SYBR Green Quantitative PCR kit from Bio-Rad in a MyiQ Cycler following the manufacturer's protocol. Amplification was carried out in a total volume of 20 μL for 40 cycles of 15 seconds at 95°C, 20 seconds at 60°C, and 30 seconds at 72°C. Samples were run in triplicate and their relative expression was determined by normalizing expression of each target either to GAPDH or β-actin. These were then compared with the normalized expression in a reference sample to calculate a fold change value. Primers were designed as described previously (26). Primer sequences were as follows: human GAPDH 5′-TGCACCACCAACTGCTTAGC-3′ and 5′-GGCATGGACTGTGGTCATGAG-3′, β-actin 5′-GATGAGATTGGCATGGCTTT-3′ and 5′-CACCTTCACCGTTCCAGTTT-3′, human E-cadherin 5′-CGGGAATGCAGTTGAGGATC-3′ and 5′AGGATGGTGTAAGCGATGGC-3′, human ZEB1 5′-AGCAGTGAAAGAGAAGGGAATGC-3′ and 5′-GGTCCTCTTCAGGTGCCTCAG-3′, and human Snail 5′-CGCGCTCTTTCCTCGTCAG-3′and 5′TCCCAGATGAGCATTGGCAG-3′.

Electrophoretic mobility shift assay. Preparation of nuclear extracts and electrophoretic mobility shift assay (EMSA) experiments were done as described previously (27) with minor modifications. Control and PGE_2-treated (2 μg/mL) A549 cells were lysed in 0.5% NP40 and centrifuged to pellet the nuclei. Nuclear proteins were then extracted in 20 mmol/L HEPES (pH 7.6), 25% glycerol, 840 mmol/L KCl, 1.5 mmol/L $MgCl_2$, 0.2 mmol/L EDTA, 0.5 mmol/L DTT, and a standard protease inhibitor cocktail. The double-stranded oligonucleotide used as a probe for EMSA experiments corresponds to the following sequence in the E-cadherin promoter: E-box-3 (positions +10 to +38), 5′-GGAACTGAAAG*C*ACCT*G*TGAGCTTGCGG (28). The two italicized residues of the indicated oligonucleotides were changed to A in the mutated versions used in the competition experiments. Probes were labeled with [γ-^{32}P]ATP and polynucleotide kinase and then purified using a spin column (Bio-Rad). Reactions with equal amounts of nuclear extracts (10 μg/reaction) were performed in a 20 μL final volume containing binding buffer [20 mmol/L HEPES (pH 7.6), 150 mmol/L KCl, 3 mmol/L $MgCl_2$, 10% glycerol, 0.2 mmol/L $ZnSO_4$, 0.3 mg/mL bovine serum albumin],

50,000 cpm probe, and 1 μg poly(deoxyinosinic-deoxycytidylic acid) for 30 minutes at 4°C. For competition assays, 200-fold unlabeled oligonucleotides were preincubated with cell extracts at 4°C for 30 minutes before addition of probe. Complexes were resolved on 5% nondenaturing polyacrylamide gels in Tris borate-EDTA buffer.

Chromatin immunoprecipitation assay. Chromatin immunoprecipitation analysis was performed utilizing the ChIP-IT Enzymatic kit (Active Motif, Carlsbad, CA) following the manufacturer's protocol. Briefly, A549 cells, control and PGE_2 treated, were grown to 70% to 80% confluence on 100 mm dishes. The cells were first fixed with 1.0% formaldehyde and used for chromatin preparation as described in the manufacturer's protocol. Chromatin were then precleared with protein G beads for 2 hours at 4°C. Antibodies to ZEB-C (COOH terminal), anti-ZEB-N (NH_2 terminal), Snail, and control IgG (normal goat IgG) were then added to the precleared chromatin and incubated overnight at 4°C. Subsequently, protein G beads were added to the immunoprecipitated chromatin DNA and incubated for 1.5 hours at 4°C. The beads were then collected by centrifugation and washed extensively. The cross-linked DNA was then eluted from protein G beads. The eluted cross-linked protein-DNA complexes were treated with RNase A at 65°C overnight for the removal of RNA and then treated with proteinase K at 42°C for 2 hours to reverse protein-DNA complex. The resulting DNA was purified by columns and then subjected to PCR analysis. PCRs were done with the following human E-cadherin promoter primers: forward 5′-GGCCGGCAGGTGAACCCTCA-3′ and reverse 5′-GGGCTGGAGTCTGAACTGA-3′ (accession no. L34545; ref. 28).

Small interfering RNA–mediated RNA interference. To inhibit ZEB1 expression, A549 cells were transfected with validated small interfering RNA (siRNA) ZEB188 or scrambled control ZEB188 siRNA (26). ZEB188 siRNA duplex was obtained from Ambion (Austin, TX). Effective sequences were selected as described earlier (26); sequences are as follows: ZEB188 (sense) 5′-UGAUCAGCCUCAAUCUGCAtt-3′, ZEB188 (antisense) 5′-UGCAGAUUGAGGCUGAUCAtt-3′, ZEB188 scramble (sense) 5′-UGACUGAGUGCGAUCAUGAtt-3′, and ZEB188 scramble (antisense) 5′-UCAUGAUCGCACUCAGUCAtt-3′. To inhibit Snail expression, A549 cells were transfected with validated siRNA for Snail or green fluorescent protein (siRNA) as control (27, 29). The Snail siRNA duplex was obtained from Dharmacon (Lafayette, CO). The target sequences were selected as described previously (27, 29). Sequences are as follows: Snail (5′-GCGAGCUGCAGGACUCUAA-3′) and GFP (5′-GGCTACGTCCAGGAGCGCACC-3′). A549 cells (1×10^5-2.5×10^5) were seeded in six-well plates in 10% FBS-containing RPMI. Twenty-four hours later, 20 nmol/L siRNA for either ZEB1 or Snail was transfected using SiLentFect Lipid reagent (Bio-Rad) following the manufacturer's instructions. Cell density was 60% to 75% confluence at the time of transfection. PGE_2 (10 μg/mL) was added to the culture following a 6-hour incubation with ZEB1 siRNA. At 24 hours post-transfection, total RNA was prepared using TRIzol reagent according to the manufacturer's instructions. In Snail siRNA experiments, PGE_2 (10 μg/mL) was added to the culture following a 72-hour incubation with Snail siRNA. At 96-hour post-transfection, total RNA was prepared as described above. GAPDH siRNA (20 nmol/L, Ambion) was used as a positive control and silencer siRNA (20 nmol/L, Ambion) was used as negative control.

Immunohistochemistry. With institutional review board approval, immunohistochemistry was performed utilizing formalin-fixed, paraffin-embedded tissues from the University of California at Los Angeles (UCLA) Lung Cancer Specialized Programs of Research Excellence (SPORE) tissue bank and pathology department archives. Tissue sections (4 μm thick) were cut, deparaffinized in xylene, rehydrated in alcohols, and washed twice with water. Samples were then incubated in 0.01 mol/L citrate buffer (pH 6.0) for 25 minutes in a steamer to unmask antigens as described previously (30, 31). Following cooling to room temperature and rinsing with distilled H_2O (dH_2O), samples were treated for 15 minutes with 3% H_2O_2 diluted in methanol. Tissue sections were washed in dH_2O and then PBS and blocked with 10% normal horse serum for 30 minutes at room temperature. For COX-2 and E-cadherin costaining (n = 25), the sections were first stained for COX-2 followed by E-cadherin. The sections were incubated with goat anti-human COX-2 polyclonal IgG 1.0 μg/mL (Santa Cruz Biotechnology) overnight at 4°C, rinsed, and incubated for 40 minutes at room temperature with 7.5 μg/mL horse anti-goat IgG-biotin (Vector Laboratories, Inc., Burlingame, CA; ref. 31). Samples were then incubated for 30 minutes at room temperature, with avidin-horseradish peroxidase diluted 1:1,000 in PBS (Vector Laboratories), washed, and treated

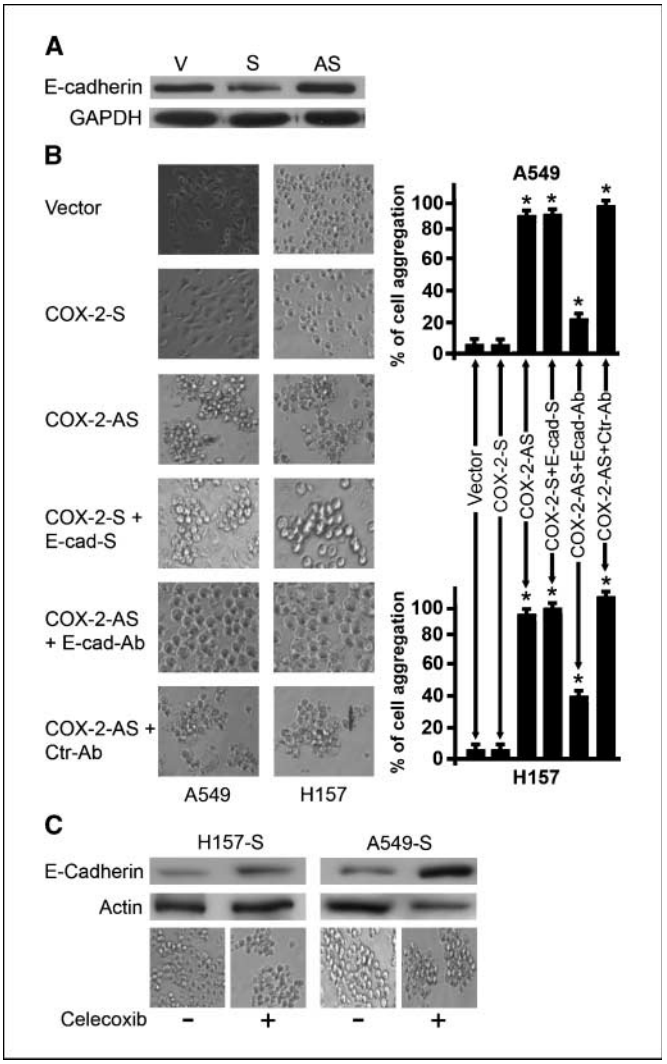

Figure 1. COX-2-dependent expression of E-cadherin and cell aggregation in NSCLC cells. The protein from whole-cell lysates of NSCLC cells [empty vector (*V*), COX-2-S (*S*), and COX-2-AS (*AS*) transfectants] was analyzed for E-cadherin expression by Western blot. *A,* A549 cells. COX-2-AS exhibits enhanced constitutive E-cadherin protein, whereas COX-2-S cells show decreased E-cadherin protein. Equal loading of protein was confirmed with anti-GAPDH antibody. Similar results were obtained with H157 cells (data not shown). *B,* NSCLC cells were used for cell aggregation assays. *Left,* A549; *right,* H157. Significantly enhanced cell aggregation was seen in COX-2-AS (90% aggregation) compared with COX-2-S and empty vector (1.0% aggregation; $P < 0.001$). Overexpression of E-cadherin in COX-2-S (*COX-2-S + E-cad-S*) cells enhanced the cell aggregation capacity in both cell lines (91% aggregation) compared with COX-2-S (1.0% aggregation) control cells ($P < 0.001$). Cell aggregation in vector control cells was indistinguishable from that seen in COX-2-S cells. Blocking E-cadherin in COX-2-AS cells with anti-E-cadherin antibody (*COX-2-AS + E-cad-Ab*) led to an 80% reduction in cell aggregation compared with COX-2-AS cells treated with control antibody (*COX-2-AS + Ctr-Ab*). *Columns,* percentage of cell aggregation in each group. Representative of the average of five fields in three independent experiments. *C,* NSCLC cells (A549-S and H157-S) were exposed to celecoxib (1 μmol/L). After 24 hours, the cells were harvested and protein from whole-cell lysates was analyzed by Western blot. An increase in E-cadherin protein and cellular aggregation was seen in celecoxib-treated cells (90% cell aggregation). Diluent-treated COX-2-S showed 1% aggregation. Equal loading of protein was confirmed with anti-actin antibody.

Table 1. COX-2-dependent regulation of E-cadherin transcriptional repressors ZEB1 and Snail in NSCLC

	Fold difference vs mock-transfected cells		
Experimental condition	ZEB mRNA	Snail mRNA	E-cadherin mRNA
Vector	1	1	1
Vector + PGE_2	1.7 ± 0.03	2.11 ± 0.8	0.3 ± 0.02
COX-2-S	1.5 ± 0.3	1.27 ± 0.2	0.4 ± 0.15
COX-2-AS	0.76 ± 0.2	0.5 ± 0.1	1.4 ± 0.5

NOTE: E-cadherin, ZEB1, and Snail expression levels were evaluated by quantitative real-time PCR analysis as described in Materials and Methods. E-cadherin mRNA levels were decreased in COX-2-S or vector cells exposed to PGE_2. ZEB1 and Snail mRNA expression levels were elevated in response to PGE_2 or COX-2 overexpression. In COX-2-AS, the E-cadherin expression level was increased, whereas ZEB1 and Snail expression was decreased. Similar results were also obtained in H157 cells (data not shown). Mean of three independent experiments.

with nickel 3,3′-diaminobenzidine (DAB kit, Vector laboratories) for black color development to augment contrasting color in double-stained slides. Samples were extensively washed in PBS (thrice, 5 minutes each) in preparation for E-cadherin staining. Samples were incubated overnight at 4°C with 250 μg/mL mouse anti-human E-cadherin diluted in normal horse serum (BD Transduction Biosciences, San Diego, CA). After extensive rinsing with PBS, samples were incubated for 40 minutes with 7.5 μg/mL horse anti-mouse IgG-biotin. Sections were rinsed with PBS, then incubated for 30 minutes at room temperature with the Vectastain ABC kit (Vector Laboratories) followed by PBS washing and then incubation with alkaline phosphatase substrate kit (Vector Laboratories). Color development was followed under the microscope for 20 minutes. The color reaction was stopped by rinsing with dH_2O. Samples were counterstained with hematoxylin. Normal human kidney was used as a positive control for both COX-2 and E-cadherin staining. Negative controls included incubation with nonimmune pooled rabbit or goat IgG (rabbit IgG was from Vector Laboratories and goat IgG was from Zymed/Invitrogen) at the same concentration as primary antibody.

Single staining for ZEB1, COX-2, and double staining for ZEB1 and E-cadherin was performed (n = 18) essentially as described above with the following modifications. Goat anti-human ZEB polyclonal IgG (1:50 dilution, Santa Cruz Biotechnology) was used for ZEB1 immunohistochemistry.

All slides were reviewed by two of the investigators (M.C.F. and C.L.). The following findings were recorded for each slide: (*a*) % cells positive for each stain (E-cadherin, COX-2, and ZEB1), (*b*) intensity of stain (0 to +3); (*c*) pattern of staining (membranous, cytoplasmic, and nuclear); and (*d*) in slides that had double staining, the percentage of cells that showed coexpression of both antigens (E-cadherin and COX-2 or E-cadherin and ZEB1).

Results and Discussion

COX-2-dependent expression of E-cadherin and cell aggregation in NSCLC cells. Previous studies support the relationship between COX-2 and its synthesized product PGE_2 to the neoplastic transformation of epithelial cells (32–34). COX-2 expression is constitutively up-regulated in several different malignancies, including lung cancer (2–5). Our previous studies documented a tumor COX-2-dependent regulation of CD44- and MMP-2-mediated invasion in NSCLC that occurs via PGE_2-EP receptor signaling (14, 15).

In addition to invasion of ECM, tumor cell homotypic adhesion is important in cellular aggregation and thus metastatic potential. Epithelial-mesenchymal transition (EMT), a process associated with loss of epithelial polarity and cell-cell adhesion, has been found to be operative in both embryonic development and carcinogenesis (35, 36). Loss of E-cadherin, a major hallmark of the EMT process, is frequently observed at sites of EMT during cancer development and progression (37). Reduced E-cadherin expression has been reported

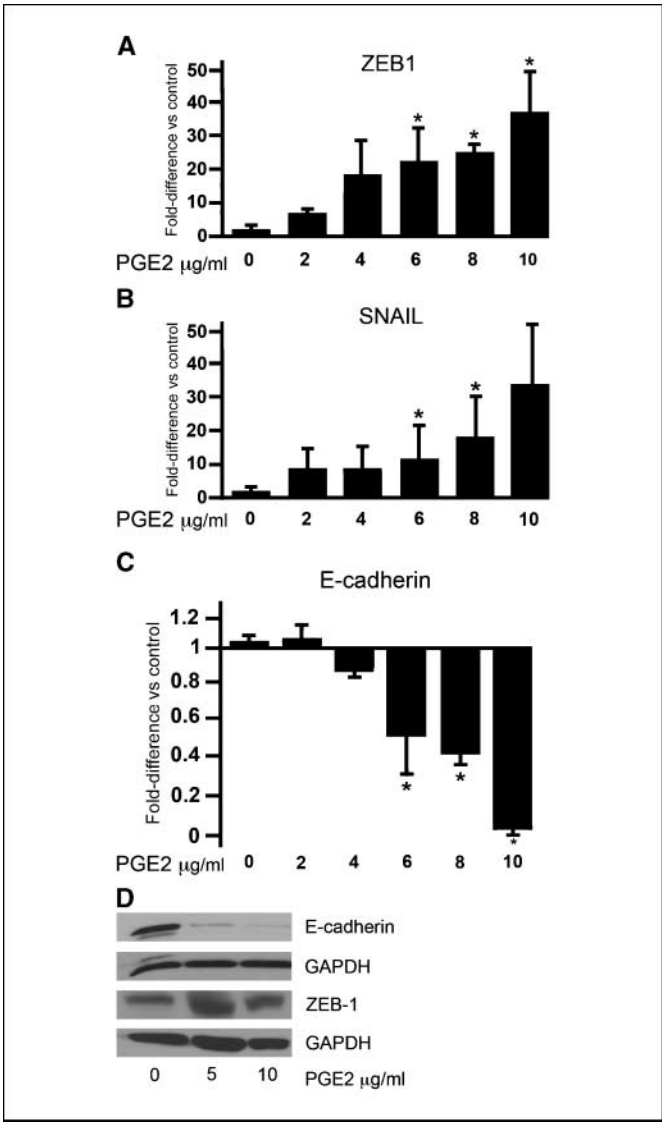

Figure 2. PGE_2-dependent regulation of E-cadherin, ZEB1, and Snail in NSCLC. PGE_2 regulates expression of E-cadherin and its transcriptional repressors ZEB1 and Snail in a dose-dependent manner. A549 cells were treated with the indicated concentrations of PGE_2 for 18 hours and levels of mRNA for E-cadherin, ZEB1, and Snail were evaluated by quantitative real-time PCR analysis as described in Materials and Methods. *A,* a PGE_2 dose-dependent increase in ZEB1 was shown in NSCLC cells (*, $P \leq 0.05$, a significant increase compared with control untreated cells). *B,* a PGE_2 dose-dependent increase in Snail was shown in NSCLC cells (*, $P \leq 0.05$, a significant increase compared with control untreated cells). *C,* a PGE_2 dose-dependent decrease in E-cadherin was shown in NSCLC cells (*, $P \leq 0.05$, a significant decrease compared with control untreated cells). *D,* Western blot analysis of NSCLC (H157) cells show decreased E-cadherin and increased ZEB1 protein in PGE_2-treated cells (24 hours).

Table 2. Inhibition of ZEB1 or Snail interrupts the PGE_2-mediated down-regulation of E-cadherin in NSCLC

	Fold difference vs mock-transfected cells	
Treatment	ZEB1 or SNAIL mRNA	E-cadherin mRNA
Control siRNA	1	1
ZEB-siRNA	0.50 ± 0.12	7.0 ± 1
Control siRNA + PGE_2	4.27 ± 0.12	0.20 ± 0.12
ZEB-siRNA + PGE_2	0.35 ± 0.02	3.3 ± 0.07
Control siRNA	1	1
Snail-siRNA	0.79 ± 0.09	29 ± 11
Control siRNA + PGE_2	6.0 ± 1.0	0.3 ± 0.02
Snail-siRNA + PGE_2	0.35 ± 0.02	10.5 ± 3.5

NOTE: E-cadherin, ZEB1, and Snail expression levels were evaluated by quantitative real-time PCR analysis as described in Materials and Methods. In control siRNA-treated cells exposed to PGE_2 (10 μg/mL), E-cadherin mRNA levels were decreased (0.20-fold), whereas ZEB1 mRNA was increased (4.27-fold). siRNA-mediated knockdown of ZEB1 expression decreased ZEB1 mRNA (0.50-fold) and increased E-cadherin mRNA expression (7.0-fold). siRNA-mediated knockdown of ZEB1 expression interrupted the PGE_2-mediated down-regulation of E-cadherin mRNA expression. Similarly, in control siRNA-treated cells exposed to PGE_2 (10 μg/mL), E-cadherin mRNA expression was decreased (0.3-fold) and Snail mRNA increased (6.0-fold). Knockdown with Snail siRNA decreased Snail mRNA (0.79-fold) and increased E-cadherin mRNA expression (29.0-fold). siRNA-mediated knockdown of Snail expression interrupted the PGE_2-mediated down-regulation of E-cadherin mRNA expression. Mean ± SD of triplicate determinations in a representative experiment of three separate experiments.

to occur in a variety of malignancies and is closely correlated with tumor invasion and metastasis (38, 39). Tumor cells with limited E-cadherin expression are more likely to detach from a tumor mass than are high E-cadherin-expressing tumor cells (40), thus suggesting a mechanism whereby limited cell-cell adhesion could lead to tumor metastasis (22).

To evaluate the role of E-cadherin expression in COX-2-dependent lung cancer cellular aggregation, we determined the level of E-cadherin in COX-2-transduced NSCLC cell lines. As we have described previously (14), COX-2-S cells produced significantly more PGE_2 (at least 10-fold greater than vector only controls). Here, we found that COX-2-S cells showed down-regulation of E-cadherin (Fig. 1*A*) and showed limited capacity for cellular aggregation compared with controls (Fig. 1*B*). In contrast, COX-2-AS cells produced less PGE_2 (14), expressed high level E-cadherin (Fig. 1*A*), and showed an enhanced capacity for cellular aggregation (Fig. 1*B*). To assess the effect of COX-2-dependent regulation of E-cadherin, COX-2-S cells were transduced with a human E-cadherin-expressing retroviral vector. Two transfected cell lines, A549-COX-2-S-E-cadherin and H157-COX-2-S-E-cadherin, were tested for cell aggregation in comparison with the COX-2-S cells. As depicted in Fig. 1*B*, overexpression of E-cadherin in COX-2-S cells significantly enhanced their cellular aggregation capacity. Moreover, blocking E-cadherin expression in COX-2-AS cells with anti-E-cadherin antibody significantly reduced the cellular aggregation capacity (Fig. 1*B*). In contrast, control antibody did not alter cell aggregation (Fig. 1*B*). The percentage of cell aggregation in each group is shown in the bar graph (Fig. 1*B*). These findings suggest that E-cadherin expression and cellular aggregation in NSCLC are COX-2 dependent.

In accord with the results described above, it has been shown that a COX-2 inhibitor up-regulated E-cadherin expression in colon cancer cell lines (41). COX-2 inhibitors are currently being evaluated in clinical chemoprevention and therapy trials for NSCLC (18). Thus, COX-2-dependent regulation of E-cadherin could eventually be one pathway for targeting and evaluation of response in clinical studies. Therefore, the effect of celecoxib was assessed in A549-S and H157-S cells. Consistent with our findings in COX-2-AS cells, celecoxib (1 μmol/L) increased E-cadherin expression and cellular aggregation in COX-2-S cells (Fig. 1*C*). Thus, these results implicate COX-2/PGE_2 as an important inhibitor of E-cadherin expression in NSCLC and suggest a role for pharmacologic inhibition of COX-2 in regulating this response.

COX-2-dependent up-regulation of the E-cadherin transcriptional repressors, ZEB1 and Snail, in NSCLC. Based on the above findings, we sought to determine how COX-2/PGE_2 regulates E-cadherin expression in NSCLC. Although inactivating mutations or promoter hypermethylation have been observed to account for loss of E-cadherin function in some malignancies,

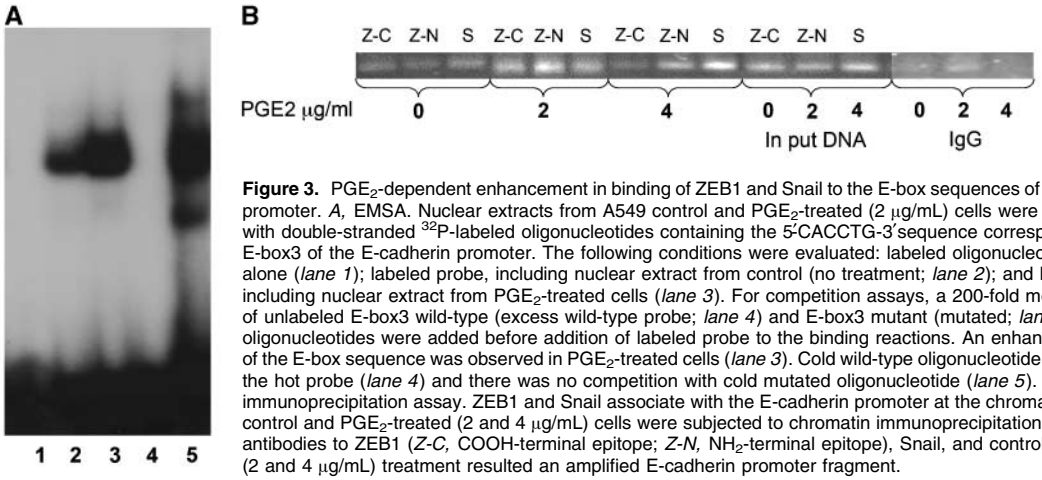

Figure 3. PGE_2-dependent enhancement in binding of ZEB1 and Snail to the E-box sequences of the E-cadherin promoter. *A,* EMSA. Nuclear extracts from A549 control and PGE_2-treated (2 μg/mL) cells were incubated with double-stranded ^{32}P-labeled oligonucleotides containing the 5′CACCTG-3′sequence corresponding to E-box3 of the E-cadherin promoter. The following conditions were evaluated: labeled oligonucleotide probe alone (*lane 1*); labeled probe, including nuclear extract from control (no treatment; *lane 2*); and labeled probe, including nuclear extract from PGE_2-treated cells (*lane 3*). For competition assays, a 200-fold molar excess of unlabeled E-box3 wild-type (excess wild-type probe; *lane 4*) and E-box3 mutant (mutated; *lane 5*) oligonucleotides were added before addition of labeled probe to the binding reactions. An enhanced binding of the E-box sequence was observed in PGE_2-treated cells (*lane 3*). Cold wild-type oligonucleotide competed with the hot probe (*lane 4*) and there was no competition with cold mutated oligonucleotide (*lane 5*). *B,* chromatin immunoprecipitation assay. ZEB1 and Snail associate with the E-cadherin promoter at the chromatin level. A549 control and PGE_2-treated (2 and 4 μg/mL) cells were subjected to chromatin immunoprecipitation analysis using antibodies to ZEB1 (*Z-C,* COOH-terminal epitope; *Z-N,* NH_2-terminal epitope), Snail, and control IgG. PGE_2 (2 and 4 μg/mL) treatment resulted an amplified E-cadherin promoter fragment.

transcriptional repression has emerged as one of the important mechanisms for the down-regulation of E-cadherin expression during tumor development and progression (26, 35, 37). Recently, several E-cadherin transcriptional repressors have been characterized (ZEB1, Snail, E12/E47, Slug, Twist, and SIP-1) and shown to interact with proximal E-boxes of the E-cadherin promoter (26, 35, 37, 42, 43).

As reported previously (44), among these repressors, ZEB1 and Snail expression was significantly correlated with reduced expression of E-cadherin and EMT transition in tumor cells. In addition, ZEB1 expression has been shown to reduce the expression of E-cadherin in NSCLC cells (26). Here, we determined whether COX-2/PGE_2 could regulate ZEB1 and Snail and thus reduce the expression of E-cadherin in NSCLC cells. We quantified ZEB1, Snail, and E-cadherin expression by real-time RT-PCR in COX-2-S, COX-2-AS, and PGE_2-treated vector control cells. In COX-2-S cells exposed to medium alone or vector cells exposed to PGE_2, ZEB1 and Snail mRNA expression levels were elevated. Consistent with these findings, E-cadherin mRNA expression was decreased under these conditions (Table 1). As determined by quantitative real-time PCR, PGE_2 down-regulated E-cadherin and up-regulated its transcriptional repressors, ZEB1 and Snail, in a dose-dependent manner (Fig. 2*A-C*). PGE_2-mediated up-regulation of ZEB1 and down-regulation of E-cadherin were also observed by Western blot analysis (Fig. 2*D*).

To determine the importance of ZEB1 and Snail in the PGE_2-mediated down-regulation of E-cadherin, we used siRNA to knockdown ZEB1 and Snail expression in A549 cells (Table 2). Transfection with ZEB188 siRNA resulted in a 0.5-fold reduction of ZEB1 mRNA levels compared with mock-transfected cells (Table 2). Concomitantly, siRNA-mediated knockdown of ZEB1 led to 7.0-fold increase in E-cadherin mRNA level (Table 2). Treatment of A549 cells with PGE_2 increased ZEB1 mRNA expression (4.27-fold) and decreased the E-cadherin mRNA level. Knockdown of ZEB1 expression interrupted the PGE_2-mediated down-regulation of E-cadherin (Table 2). Transfection with Snail siRNA resulted in a 0.79-fold reduction of Snail mRNA levels compared with mock-transfected cells (Table 2). Concomitantly, siRNA-mediated knockdown of Snail led to 29.0-fold increase in E-cadherin mRNA (Table 2). Treatment of A549 cells with PGE_2 increased Snail mRNA 6.0-fold and decreased E-cadherin mRNA expression 0.3-fold. Knockdown of Snail expression interrupted the PGE_2-mediated down-regulation of E-cadherin (Table 2). These findings implicate PGE_2 as an autocrine or paracrine modulator of ZEB1 and Snail and define a pathway by which COX-2 decreases E-cadherin expression in NSCLC.

ZEB1 and Snail bind to E-box elements of the E-cadherin promoter. ZEB1 and Snail are known to bind the E-boxes present in the E-cadherin promoter and thus repress E-cadherin transcription (27, 28). To test whether the PGE_2-mediated elevation in ZEB1 and Snail is associated with an increase in binding to the E-cadherin

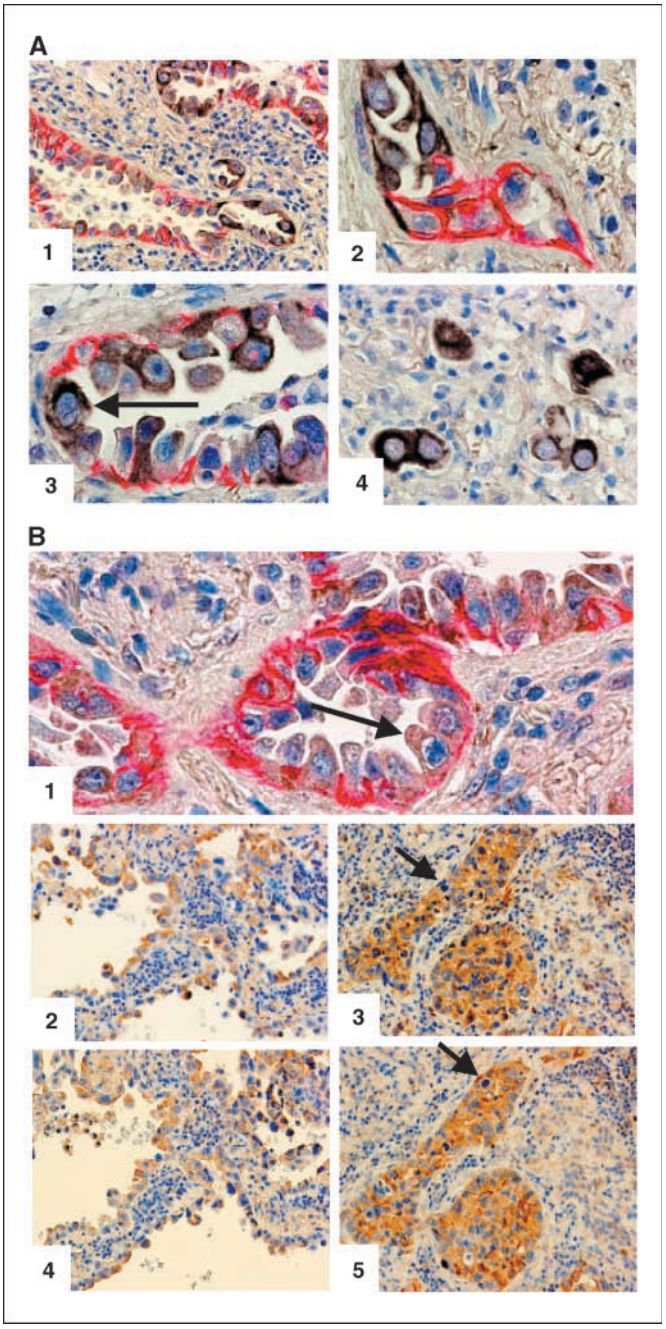

Figure 4. Distinct patterns of COX-2, E-cadherin, and ZEB expression in NSCLC. *A, 1* to *4,* distinct patterns of COX-2 and E-cadherin expression in NSCLC. COX-2 and E-cadherin expression in paraffin-embedded sections of human lung adenocarcinoma surgical specimens were assessed by immunohistochemistry using a double-staining method. Lung adenocarcinoma cells positive for COX-2 stain dark brown and E-cadherin-positive cells stain red. Interstitial cells and ECM did not stain significantly for either COX-2 or E-cadherin. *1,* when there was high expression of COX-2 (*black*) in a neoplastic cell, there was most often low expression of E-cadherin (*red*). *2,* within a group of malignant cells, a portion of tumor cells stains for COX-2 and another portion of adjacent tumor cells stain for E-cadherin. *3,* with coexpression of COX-2 and E-cadherin, the COX-2 staining is intense in cells that did not costain for E-cadherin. *4,* individual, discohesive infiltrating cells stain primarily for COX-2. The percentage of tumor cells, which coexpress significant levels of both COX-2 and E-cadherin, is negligible. Magnification, ×100 (*1*) and ×400 (*2-4*). *B, 1* to *5,* distinct patterns of ZEB1 and E-cadherin expression in NSCLC. ZEB1, COX-2, and E-cadherin expression was assessed by immunohistochemistry in paraffin-embedded sections of human lung adenocarcinoma surgical specimens. Lung adenocarcinoma cells positive for COX-2 and ZEB1 stain brown and E-cadherin-positive cells stain red. *1,* double immunohistochemical staining for E-cadherin (*red*) and ZEB1 (*brown*) showing reciprocal relationship. *Arrows,* examples of ZEB1-positive, E-cadherin-negative cells. Single immunohistochemical staining of low-grade adenocarcinoma with bronchioloalveolar features showing relatively mild staining for ZEB1 (*2*) and Cox-2 (*4*). Single immunohistochemical staining of high-grade adenocarcinoma with solid pattern showing strong staining for ZEB1 (*3*) and Cox-2 (*5*). Magnification, ×400 (*1*) and ×200 (*2-5*).

promoter, we examined the binding of these transcriptional repressors to E-boxes in EMSA and chromatin immunoprecipitation studies. First, nuclear extracts from control and PGE_2-treated A549 cells were used to assess binding of E-box sequences in the E-cadherin promoter. We generated oligonucleotide probes as described previously (28) comprising the E-box binding sequences *C*ACCT*G*. We also generated a control probe in which binding sequences of the E-cadherin promoter are mutated into *A*ACCT*A* (where C and G are mutated to A; ref. 28). No band was evident when the labeled oligonucleotide was used without nuclear lysate (Fig. 3*A*, *lane 1*, probe alone). In contrast, inclusion of nuclear lysate from control untreated cells clearly shows a retarded electrophoretic mobility band (Fig. 3*A, lane 2*). Compared with the untreated control cells (Fig. 3*A, lane 2*) following PGE_2 exposure, an increase in the intensity of the retarded band is shown (Fig. 3*A, lane 3*). Furthermore, use of excess unlabeled probe (Fig. 3*A, lane 4*) specifically competed with the shifted band as shown in *lane 3*. However, a mutant probe in which the E-box was altered showed no competition (Fig. 3*A, lane 5*). These findings are consistent with those reported previously, showing Snail binding to E-boxes of the E-cadherin promoter (28). Further, to show ZEB1 and Snail interacts directly with the endogenous E-cadherin promoter, we performed chromatin immunoprecipitation experiments as described previously (45). In accord with previous findings (45) anti-ZEB1 antibody directed against the NH_2-terminal domain efficiently pulled down ZEB1 protein complexes with the chromatin fragment comprising the −84 to +60 E-cadherin promoter region (Fig. 3*B*). Similarly, an antibody directed to Snail pulled down Snail protein complexes with the same size chromatin fragment as seen for ZEB1 (−84 to +64; Fig. 3*B*). An antibody against ZEB1 COOH terminal was weakly effective in immunoprecipitation, whereas control goat IgG did not precipitate the E-cadherin promoter region (Fig. 3*B*). Importantly, an enhanced expression of ZEB1 and Snail in PGE_2-treated cells resulted in an increase in chromatin binding as shown by the increase in intensity of the band in Fig. 3*B*. The sequence analysis of the amplified promoter fragments of ZEB1 and Snail-precipitated chromatin from the PCR confirmed the binding of these transcriptional inhibitors to the E-boxes of the E-cadherin promoter (data not shown).

Expression of COX-2, ZEB1, and E-cadherin in human NSCLC tissue sections. Reduction or loss of E-cadherin expression together with increased COX-2 expression has been reported previously in colorectal and gastrointestinal neoplasms (16). Based on our *in vitro* findings in NSCLC cell lines, we sought to determine if the reciprocal expression of E-cadherin and COX-2 was evident in NSCLC cells *in situ*. Twenty-five paraffin-embedded lung adenocarcinomas were assessed for COX-2 and E-cadherin expression by a double-staining immunohistochemistry method. Reciprocal expression of COX-2 and E-cadherin in human NSCLC tissue sections was evident (Fig. 4); when there was expression of COX-2 (black staining) in a neoplastic cell, there most often was no expression of E-cadherin (red staining) as seen in Fig. 4*A, 1*. Commonly, when NSCLC cells expressed E-cadherin, they did not express COX-2 (Fig. 4*A, 2*). Within the same neoplasm, some NSCLC cells stained for COX-2, whereas adjacent tumor cells stained for E-cadherin (Fig. 4*A, 2* and *3*). In double-stained slides, coexpression of E-cadherin on the cell membrane and COX-2 in the cytoplasm occurred only in 3.75 ± 8.8% of neoplastic cells. Indeed, as predicted from our *in vitro* data (Fig. 1), the strongest staining for COX-2 occurred in individual, discohesive infiltrating neoplastic cells (Fig. 4*A, 4*). There was great variability in COX-2 and E-cadherin expression from one tumor to another and within the neoplastic tissue of each tumor. When findings in low-grade verses high-grade neoplasms were compared, higher-grade neoplasms showed greater expression of COX-2 and less expression of E-cadherin than low-grade neoplasms. These findings are consistent with differential expression of these two proteins shown *in vitro* (Fig. 1) as well as a previous report in rat intestinal epithelial cells (23).

The COX-2-dependent reciprocal expression of ZEB1 and E-cadherin observed *in vitro* (Table 1) prompted us to determine if this relationship is also present in human neoplasm sections obtained from surgical specimens. Reciprocal expression of ZEB1 and E-cadherin in histologic sections of human NSCLC was evident (Fig. 4*B, 1*) in a manner analogous to that seen with E-cadherin and COX-2 staining (Fig. 4*A, 1-4*). Only 4.17 ± 9.5% of cells expressed both ZEB1 and E-cadherin. Low-grade adenocarcinomas showed much less expression of ZEB1 (Fig. 4*B, 2*) and COX-2 (Fig. 4*B, 4*) than high-grade neoplasms. Immunohistochemical staining of high-grade adenocarcinomas with a solid pattern showed stronger staining for ZEB1 (Fig. 4*B, 3*) and COX-2 (Fig. 4*B, 5*). Consistent with our *in vitro* findings (Table 1), the examination of serial sections indicated that tumor cells that were positive for COX-2 were predominantly also ZEB1 positive. Thus, to summarize the findings of the immunohistochemical studies in human lung adenocarcinomas, there is (*a*) reciprocal expression of E-cadherin and COX-2, (*b*) reciprocal expression of E-cadherin and ZEB1, (*c*) coexpression of COX-2 and ZEB1, and (*d*) very rare coexpression of membranous E-cadherin and COX-2 or ZEB1.

Here, for the first time, we document COX-2-dependent transcriptional regulation of E-cadherin and cellular aggregation in NSCLC. Furthermore, in human lung adenocarcinomas, we confirm a reciprocal relationship between COX-2 and E-cadherin as well as ZEB1 and E-cadherin. The studies presented here also indicate a positive correlation between COX-2 and ZEB1 in human lung adenocarcinomas. These findings suggest that therapies targeting the COX pathway may diminish the propensity for tumor metastasis in NSCLC by blocking the PGE_2-mediated induction of E-cadherin transcriptional repressors. This newly defined pathway for transcriptional regulation of E-cadherin in NSCLC has important implications for chemoprevention as well as therapies using COX-2 inhibitors in combination with other agents. For example, E-cadherin expression in NSCLC cells has recently been implicated as a marker of sensitivity to epidermal growth factor receptor (EGFR) tyrosine kinase inhibitors (TKI; refs. 46–49). Thus, COX-2 inhibitors enhance tumor E-cadherin expression and may therefore augment sensitivity to EGFR TKI therapy. This is now being assessed in lung cancer clinical trials (46, 50). Therefore, blocking PGE_2 production or activity may prove to be beneficial in chemoprevention and/or therapy of NSCLC.

Acknowledgments

Received 10/10/2005; revised 2/28/2006; accepted 3/8/2006.

Grant support: UCLA Lung Cancer SPORE grant P50 CA90388, Colorado Lung Cancer SPORE grant CA58187, American Lung Association, Merit Review Research Funds from the Department of Veterans Affairs, and Tobacco-Related Disease Research Program of the University of California.

The costs of publication of this article were defrayed in part by the payment of page charges. This article must therefore be hereby marked *advertisement* in accordance with 18 U.S.C. Section 1734 solely to indicate this fact.

We thank Dr. Young Whan Kim for critical review of the article and Dr. Ayyappan K. Rajasekaran for valuable suggestions.

References

1. Brown JR, DuBois RN. Cyclooxygenase as a target in lung cancer. Clin Cancer Res 2004;10:4266–9s.
2. Dubinett SM, Sharma S, Huang M, Dohadwala M, Pold M, Mao JT. Cyclooxygenase-2 in lung cancer. Prog Exp Tumor Res 2003;37:138–62.
3. Dannenberg AJ, Subbaramaiah K. Targeting cyclooxygenase-2 in human neoplasia: rationale and promise. Cancer Cell 2003;4:431–6.
4. Dannenberg AJ, Zakim D. Chemoprevention of colorectal cancer through inhibition of cyclooxygenase-2. Semin Oncol 1999;26:499–504.
5. Huang M, Stolina M, Sharma S, et al. Non-small cell lung cancer cyclooxygenase-2 dependent regulation of cytokine balance in lymphocytes and macrophages: up-regulation of interleukin 10 and down-regulation of interleukin 12 production. Cancer Res 1998;58:1208–16.
6. Hilda T, Yatabe Y, Achiwa H, et al. Increased expression of cyclooxygenase 2 occurs frequently in human lung cancers, specifically in adenocarcinomas. Cancer Res 1998;58:3761–4.
7. Wolff H, Saukkonen K, Anttila S, Karjalainen A, Vainio H, Ristimaki A. Expression of cyclooxygenase-2 in human lung carcinoma. Cancer Res 1998;48:4997–5001.
8. Stolina M, Sharma S, Lin Y, et al. Specific inhibition of cyclooxygenase 2 restores antitumor reactivity by altering the balance of IL-10 and IL-12 synthesis. J Immunol 2000;165:361–70.
9. Pold M, Zhu L, Sharma S, et al. Cyclooxygenase-2-dependent expression of angiogenic CXC chemokines ENA-78/CXC ligand (CXCL) 5 and interleukin-8/CXCL8 in human non-small cell lung cancer. Cancer Res 2004;64:1853–60.
10. Tsujii M, Kawano S, Tsuji S, Sawaoka H, Hori M, Dubois R. Cyclooxygenase regulates angiogenesis induced by colon cancer cells. Cell 1998;93:705–16.
11. Sharma S, Yang SC, Zhu L, et al. Tumor cyclooxygenase-2/prostaglandin E_2-dependent promotion of FOXP3 expression and $CD4^+CD25^+$ T regulatory cell activities in lung cancer. Cancer Res 2005;65:5211–20.
12. Sharma S, Zhu L, Yang SC, et al. Cyclooxygenase 2 inhibition promotes IFN-γ-dependent enhancement of antitumor responses. J Immunol 2005;175:813–9.
13. Tsujii M, Kawano S, DuBois R. Cyclooxygenase-2 expression in human colon cancer cells increases metastatic potential. Proc Natl Acad Sci U S A 1997;94:3336–40.
14. Dohadwala M, Luo J, Zhu L, et al. Non small cell lung cancer cyclooxygenase-2-dependent invasion is mediated by CD44. J Biol Chem 2001;276:20809–12.
15. Dohadwala M, Batra RK, Luo J, et al. Autocrine/paracrine prostaglandin E_2 production by non-small cell lung cancer cells regulates matrix metalloproteinase-2 and CD44 in cyclooxygenase-dependent invasion. J Biol Chem 2002;277:50828–33.
16. Jungck M, Grunhage F, Spengler U, et al. E-cadherin expression is homogeneously reduced in adenoma from patients with familial adenomatous polyposis: an immunohistochemical study of E-cadherin, β-catenin and cyclooxygenase-2 expression. Int J Colorectal Dis 2004;19:438–45.
17. Achiwa H, Yatabe Y, Hilda T, et al. Prognostic significance of elevated cyclooxygenase 2 expression in primary, resected lung adenocarcinomas. Clin Cancer Res 1999;5:1001–5.
18. Riedl K, Krysan K, Pold M, et al. Multifaceted roles of cyclooxygenase-2 in lung cancer. Drug Resist Updat 2004;7:169–84.
19. Cavallaro U, Christofori G. Cell adhesion and signaling by cadherins and Ig-CAMs in cancer. Nat Rev Cancer 2004;4:118–32.
20. Choi YS, Shim YM, Kim SH, et al. Prognostic significance of E-cadherin and β-catenin in resected stage I non-small cell lung cancer. Eur J Cardiothorac Surg 2003;24:441–9.
21. Bremnes RM, Veve R, Gabrielson E, et al. High-throughput tissue microarray analysis used to evaluate biology and prognostic significance of the E-cadherin pathway in non-small cell lung cancer. J Clin Oncol 2002;20:2417–28.
22. Kase S, Sugio K, Yamazaki K, Okamoto T, Yano T, Sugimachi K. Expression of E-cadherin and β-catenin in human non-small cell lung cancer and the clinical significance. Clin Cancer Res 2000;6:4789–96.
23. Tsujii M, DuBois R. Alterations in cellular adhesion and apoptosis in epithelial cells overexpressing prostaglandin endoperoxide synthase-2. Cell 1995;83:493–501.
24. Liu D, Huang C, Kameyama K, et al. E-cadherin expression associated with differentiation and prognosis in patients with non-small cell lung cancer. Ann Thorac Surg 2001;71:949–51; discussion 954–45.
25. Rozanov Dv, Deryugina EI, Monosov EZ, Marchenko ND, Strongin AY. Aberrant, persistent inclusion into lipid rafts limits the tumorigenic function of membrane type-1 matrix metalloproteinase in malignant cells. Exp Cell Res 2004;283:81–95.
26. Ohira T, Gemmill RM, Ferguson K, et al. WNT7a induces E-cadherin in lung cancer cells. Proc Natl Acad Sci U S A 2003;100:10429–34.
27. Espineda CE, Chang JH, Twiss J, Rajasekaran SA, Rajasakaran AK. Repression of Na,K-ATPase β1-subunit by the transcription factor snail in carcinoma. Mol Biol Cell 2004;15:1364–73.
28. Batlle E, Sancho E, Franci C, et al. The transcription factor snail is a repressor of E-cadherin gene expression in epithelial tumour cells. Nat Cell Biol 2000;2:84–9.
29. fujita N, Jaye DL, Kajita M, Geigerman C, Moreno CS, Wade PA. MTA3 a Mi-2/NuRD complex subunit, regulates an invasive growth pathway in breast cancer. Cell 2003;113:207–19.
30. Sarantopoulos GP, Gui D, Shintaku P, et al. Immunohistochemical analysis of lung carcinomas with pure or partial bronchioloalveolar differentiation. Arch Pathol Lab Med 2004;128:406–14.
31. Krysan K, Merchant FH, Zhu L, et al. COX-2 dependent stabilization of surviving in non-small cell lung cancer. FASEB J 2004;18:206–8.
32. Chang SH, Liu CH, Conway R, et al. Role of prostaglandin E_2-dependent angiogenic switch in cyclooxygenase 2-induced breast cancer progression. Proc Natl Acad Sci U S A 2004;101:591–6.
33. Sheng H, Shaw J, Morrow JD, Beauchamp RD, DuBois RN. Modulation of apoptosis and Bcl-2 expression by prostaglandin E_2 in human colon cancer cells. Cancer Res 1998;58:362–6.
34. Subbaramaiah K, Altorki N, Chung WJ, Mestre JR, Sampat A, Dannenberg AJ. Inhibition of cyclooxygenase-2 gene expression by p53. J Biol Chem 1999;274:10911–5.
35. Thiery JP. Epithelial-mesenchymal transitions in development and pathologies. Curr Opin Cell Biol 2003;15:740–6.
36. Foty RA, Steinberg MS. Cadherin-mediated cell-cell adhesion and tissue segregation in relation to malignancy. Int J Dev Biol 2004;48:397–409.
37. Kang Y, Massague J. Epithelial-mesenchymal transitions: twist in development and metastasis. Cell 2004;118:277–9.
38. Bremnes RM, Veve R, Hirsch FR, Franklin WA. The E-cadherin cell-cell adhesion complex and lung cancer invasion, metastasis and prognosis. Lung Cancer 2002;36:115–24.
39. Conacci-Sorrell M, Zhurinskey J, Ben-Ze'ev A. The cadherin-catenin adhesion system in signaling and cancer. J Clin Invest 2002;109:987–91.
40. Mayer B, Johnson JP, Leitl F, et al. E-cadherin expression in primary and metastatic gastric cancer: down-regulation correlates with cellular dedifferentiation and glandular disintegration. Cancer Res 1993;53:1690–5.
41. Noda M, Tatsumi Y, Tomizawa M, et al. Effects of etodolac, a selective cyclooxygenase-2 inhibitor, on the expression of E-cadherin-catenin complexes in gastrointestinal cell lines. J Gastroenterol 2002;37:896–904.
42. Kajita M, McClinic KN, Wade PA. Aberrant expression of the transcription factors snail and slug alters the response to genotoxic stress. Mol Cell Biol 2004;24:7559–66.
43. Bolos V, Peinado H, Perez-Moreno MA, Fraga MF, Esteller M, Cano A. The transcription factor Slug represses E-cadherin expression and induces epithelial to mesenchymal transitions: a comparison with Snail and E47 repressors. J Cell Sci 2003;116:499–511.
44. Guaita S, Puig I, Franci C, et al. Snail induction of epithelial to mesenchymal transition in tumor cells is accompanied by MUC1 repression and ZEB1 expression. J Biol Chem 2002;277:39209–16.
45. Eger A, Aigner K, Sonderegger S, et al. Delta EF1 is a transcriptional repressor of E-cadherin and regulates epithelial plasticity in breast cancer cells. Oncogene 2005;24:2375–85.
46. Lippman SM, Gibson N, Subbaramaiah K, Dannenberg AJ. Combined targeting of the epidermal growth factor receptor and cyclooxygenase-2 pathways. Clin Cancer Res 2005;11:6097–9.
47. Witta SE, Gemmill RM, Hirsch FR, et al. Restoring E-cadherin expression increases sensitivity to epidermal growth factor receptor inhibitors in lung cancer cell lines. Cancer Res 2006;66:944–50.
48. Thomson S, Buck E, Petti F, et al. Epithelial to mesenchymal transition is a determinant of sensitivity of non-small-cell lung carcinoma cell lines and xenografts to epidermal growth factor receptor inhibition. Cancer Res 2005;65:9455–62.
49. Yauch RL, Januario T, Eberhard DA, et al. Epithelial versus mesenchymal phenotype determines *in vitro* sensitivity and predicts clinical activity of erlotinib in lung cancer patients. Clin Cancer Res 2005;11:8686–98.
50. Reckamp KL, Kostyantyn K, Morrow JD, et al. A phase I trial to determine the optimal biologic dose of celecoxib when combined with erlotinib in advanced non-small cell lung cancer. Clinical Cancer Res. In press, 2006.